Structure of the [NiFe] Hydrogenase Active Site: Evidence for Biologically Uncommon Fe Ligands[⊥]

Anne Volbeda,[†] Elsa Garcin,[†] Claudine Piras,[†] Antonio L. de Lacey,[‡] Victor M. Fernandez,[‡] E. Claude Hatchikian,[§] Michel Frey,*[,†] and Juan Carlos Fontecilla-Camps*[,†]

Contribution from the Laboratoire de Cristallographie et de Cristallogenèse des Protéines, Institut de Biologie Structurale-Jean-Pierre-Ebel CEA-CNRS, 41 Avenue des Martyrs 38027 Grenoble Cedex-France, Instituto de Catalisis, Campus Universidad Autónoma, 28049 Madrid, Spain, and Unité de Bioénergétique et Ingéniérie des Protéines, CNRS, 31 Chemin Joseph Aiguier, 13402 Marseille Cedex 20 France

Received July 3, 1996[⊗]

Abstract: Crystallographic data on the [NiFe] hydrogenase from *Desulfovibrio gigas* are presented that provide new information on the structure and mode of action of its dihydrogen activating metal center. Recently we found this center to contain, besides Ni, a second metal ion which was tentatively assigned to Fe (Volbeda, A.; Charon, M. H.; Piras, C.; Hatchikian, E. C.; Frey, M.; Fontecilla-Camps, J. C. *Nature* **1995**, *373*, 580−587). This assignment is now unambiguously confirmed by a crystallographic analysis using 3 Å resolution X-ray data collected at wavelengths close to either side of the Fe absorption edge. Moreover, we report the structure of another crystal form of the as-purified *D. gigas* hydrogenase refined at 2.54 Å resolution, showing that the active site Fe binds three diatomic ligands. The electron density map shows an additional small peak at a position bridging the two active site metal ions, which may be assigned to some form of oxygen. This bridging oxygen species is proposed to be the signature of the inactive form of the enzyme. An infrared analysis similar to the one reported for *Chromatium vinosum* hydrogenase (Bagley, K. A.; Duin, E. C.; Roseboom, W.; Albracht, S. P. J.; Woodruff, W. H. *Biochemistry* **1995**, *34*, 5527−5535) shows the existence of three bands at exceptionally high frequencies, that shift their position in a concerted fashion depending on the redox state of the enzyme. Based on these high frequencies, the diatomic Fe ligands may be assigned to nonexchangeable triply bonded molecules, possible candidates being CO, CN^- and NO. The frequency shifts of the infrared bands suggest a redox role for the Fe center during catalysis. Based on the new crystal structure and a number of spectroscopic results, possible modes of hydrogen binding to the active site are discussed.

Introduction

The enzymes directly involved in the metabolism of the most simple of chemical compounds, molecular hydrogen, are called hydrogenases. Thanks to their activity, many microorganisms can use H_2 as an energy source (H_2 uptake) or use protons as an electron sink (H_2 production), according to the reaction: $H_2 \leftrightarrow 2H^+ + 2e^-$.[1] Recently, we have reported the 2.85 Å resolution crystal structure of the heterodimeric [NiFe] hydrogenase from the sulfate-reducing bacterium *Desulfovibrio gigas*.[2] The structure includes three iron-sulfur centers disposed along an almost straight line in the 28 kDa subunit, with a [3Fe-4S] cluster intercalated between two [4Fe-4S] clusters. The active site, which is located in the 60 kDa subunit, contains a heterodinuclear metal pair consisting of Ni and an as yet unidentified second metal ion. Here, we present direct crystallographic evidence indicating that this second metal ion is Fe and provide a more detailed description of the active site obtained from a new crystal form of the enzyme refined at 2.54 Å resolution. A remarkable feature of this site is the presence of three diatomic ligands bound to the Fe center. A recent report on high frequency IR bands detected in preparations of *Chromatium vinosum* hydrogenase[3] has prompted us to carry out a similar analysis of *D. gigas* hydrogenase, and to advance the hypothesis that the unusual IR bands are generated by the diatomic ligands.[3,4]

D. gigas hydrogenase preparations isolated under aerobic conditions are inactive. They are characterized by varying ratios of two Ni EPR signals called Ni−A and Ni−B; these preparations contain typically about 50% EPR-silent material.[5,6] The Ni−A signal is generated by an unready form of the enzyme which can be activated only after a prolonged exposure to H_2. The Ni−B signal stems from a ready form, which at physiological temperatures may be immediately activated in the presence of H_2 and low potential electron acceptors.[7] Upon activation, an EPR signal known as Ni−C develops.[5,6,8] Partial reduction of the enzyme generating the Ni−B signal yields an Ni EPR-silent intermediate called Ni−SI, whereas full reduction

[†] Institut de Biologie Structurale, Grenoble, France.
[‡] Instituto de Catálisis, Madrid, Spain.
[§] Unité de Bioénergétique et Ingéniérie des Protéines, CNRS, Marseille, France.
[⊥] Abbreviations: IR, infrared; XAS, X-ray absorption spectroscopy; EPR, electron paramagnetic resonance.
* Corresponding authors.
[⊗] Abstract published in *Advance ACS Abstracts,* November 15, 1996.
(1) Adams, M. W. W.; Mortenson, L. E.; Chen, J.-S. *Biochim. Biophys. Acta* **1981**, *594*, 105−176.
(2) Volbeda, A.; Charon, M. H.; Piras, C.; Hatchikian, E. C.; Frey, M.; Fontecilla-Camps, J. C. *Nature* **1995**, *373*, 580−587.
(3) Bagley, K. A.; Duin, E. C.; Roseboom, W.; Albracht, S. P. J.; Woodruff, W. H. *Biochemistry* **1995**, *34*, 5527−5535.
(4) Fontecilla-Camps, J. C. *JBIC* **1996**, *1*, 91−98.
(5) Fernandez, V. M.; Hatchikian, E. C.; Patil, D. S.; Cammack, R. *Biochim. Biophys. Acta*. **1986**, *883*, 145−154.
(6) Cammack, R.; Patil, D. S.; Hatchikian, E. C.; Fernandez, V. M. *Biochim. Biophys. Acta* **1987**, *912*, 98−109.
(7) Fernandez, V. M.; Hatchikian, E. C.; Cammack, R. *Biochim. Biophys. Acta*. **1985**, *832*, 69−79.
(8) Some authors call the different states Ni_u, Ni_r, and Ni_a in order to make a functional distinction between the unready (u), ready (r), and active (a) form of the enzyme.

S0002-7863(96)02270-6 CCC: $12.00

of the activated enzyme results in another Ni EPR-silent state known as Ni−R.[9,10] In this paper we report the IR characterization of two additional presumably EPR-silent forms. The three [FeS] clusters are also redox-active,[11] and, consequently, different mixtures of redox states are in thermodynamic equilibrium,[9,10] making it virtually impossible to analyze most of these states in a pure, homogeneous form.

Until recently, the active site of [NiFe] hydrogenases has been generally assumed to contain only Ni as a metal ion. Accordingly, and based on the different Ni EPR signals, redox schemes involving formal Ni oxidation states ranging from 0 to +3 were proposed.[12] However, these proposals are challenged by two observations. Firstly, the X-ray absorption edge of the Ni ion in *Thiocapsa roseopersicina* hydrogenase does not change significantly for the different redox states[13] and, in the case of *D. gigas* hydrogenase, a significant Ni edge shift has only been reported so far for Ni−R.[14] Secondly, models that propose several redox states for the Ni ion are challenged by the difficulties encountered in synthesizing Ni complexes able to display midpoint redox potentials for the Ni^{3+}/Ni^{2+} and Ni^{2+}/Ni^{+} redox couples within the narrow range, typically only a few hundred millivolts, observed for the various redox states of [NiFe] hydrogenases.[15] There exist at least two alternatives to a redox active Ni ion: ligand-based redox chemistry[16] or, as we have already suggested, a redox involvement of the second active site metal ion.[2] We will elaborate on the latter point below.

Experimental Section

Cryogenic X-ray Data Close to the Fe Edge. Data for the determination of the nature of the unidentified active site metal were collected from a single flash-cooled crystal (−150 °C) of the triclinic crystal form, previously characterized at room temperature,[2] using a Mar Research image plate system at beam line 19 of the European Synchrotron Radiation Facility (ESRF). Two data sets at 3 Å resolution were collected (Table 1), at wavelengths on both sides ($\lambda_1 = 1.733$ Å, $\lambda_2 = 1.750$ Å) of the Fe absorption edge, which was checked by measuring the X-ray fluorescence of the crystal using a wavelength scan. The diffraction data were reduced with the program DENZO.[17] An energy minimization procedure using XPLOR[18] was carried out with the λ_1 data set and the known 2.85 Å resolution atomic coordinates[2] as a starting model. Tight restraints were applied for the refinement of noncrystallographic symmetry and individual temperature factors. No manual model corrections were necessary. Refinement statistics are given in Table 2.

Structure Determination of a New Crystal Form at Low Temperature. A new, pseudo-hexagonal crystal form of an as-purified, oxidized hydrogenase preparation has yielded data to 2.54 Å resolution, collected with 0.905 Å wavelength X-rays at −150 °C on beam line 4 at the ESRF. Crystal growth conditions are the same as for the previously characterized triclinic crystals,[2] since both forms grow in the same drop. The marked increase in stability upon flash-cooling, coupled to the high brilliancy of the X-ray beam, allowed us to obtain an almost complete data set from a very small ($0.03 \times 0.1 \times 0.3$ mm^3) single crystal of the new form. Diffracted X-ray intensities were collected with an image plate detector, integrated with MOSFLM,[19] and reduced to unique structure factor amplitudes with the CCP4 crystallographic package[20] (Table 1).

Table 1. X-ray Data Statistics

form[a]	λ[b] (Å)	d[c] (Å)	N_{obs}[d]	N_u[e]	C[f] (%)	R[g] (%)
A	1.733	∞−3.0	54438	29089	94.9	6.4
A	1.750	∞−3.0	53415	28271	92.2	4.8
B	0.905	∞−2.54	296283	174383	92.5	6.6
B	0.905	2.84−2.54	72596	46322	87.4	15.1

[a] A is the first crystal form (with cell dimensions $a = 62.8$ Å, $b = 93.4$ Å, $c = 69.0$ Å, $\alpha = 89.3°$, $\beta = 102.4°$, and $\gamma = 91.0°$),[2] B the new form ($a = 112.8$ Å, $b = 113.4$ Å, $c = 133.9$ Å, $\alpha = 90.0$, $\beta = 90.0°$, and $\gamma = 120.0°$. [b] X-ray wavelength. [c] Resolution range. [d] Number of independent observations. [e] Unique reflections. [f] Data completeness. [g] $R_{merge} = \sum_{hkl}\sum_j|I_{hkl,j} - \langle I_{hkl}\rangle|/\sum_{hkl,j}\langle I_{hkl}\rangle$.

The crystal structure was solved by molecular replacement with the program AMoRe[21] (Table 2), using the 2.85 Å resolution room temperature structure of the other crystal form as the starting model. Six solutions were obtained that are related by almost perfect noncrystallographic hexagonal screw axis symmetry. The model was refined first by simulated annealing, using XPLOR,[18] and then with PROLSQ,[22] after removing 5% of the data in order to calculate R_{free}.[23] Electron density maps were calculated with σ_A weights[24] and six-fold averaged with the program DEMON/ANGEL.[25] Manual model corrections were performed with the program FRODO[26] running on an ESV20 (Evans & Sutherland, Salt Lake City, Utah, U.S.A.) computer graphics workstation. In all stages of the refinement the six-fold noncrystallographic symmetry was constrained to the molecular replacement solution, thus giving rise to a high ratio of observations to refined parameters (atomic positions and temperature factors). The resulting model is of good quality, since an analysis using the program PROCHECK[27] indicates that its deviations from "ideal" stereochemistry are similar to those expected from an average model refined at 2.0 Å resolution. From a σ_A plot,[24] the root mean square coordinate error is estimated to be 0.27 Å. A total of 89% of all residues has main chain torsion angles in the most favored regions of the ϕ-ψ plot, whereas only 0.4% (3 residues) has "disallowed" ϕ-ψ combinations. The average temperature factor of the model, including water molecules, is 9.2 Å^2.

Refinement of the Active Site. Because of the high observation-to-parameter ratio (See Table 2), we decided to refine the active site without imposing any *a priori* geometric information. In order to prevent repulsive interactions between potentially binding atoms, the van der Waals term was switched off. In this way unbiased metal−ligand bond distances and angles could be obtained. These distances were used in the final stages of refinement as weak restraints, along with the van der Waals term. Moreover, difference ($F_{obs}-F_{calc}$) maps were calculated that allowed to locate all active site atoms by omitting them from the models used to generate the F_{calc}'s. After including weak bond restraints for all the metal ligands, no significant changes were observed in the structure of the active site.

IR Spectroscopic Measurements. A freshly aerobically purified[28] *D. gigas* hydrogenase preparation was used in all experiments. The

(9) Roberts, L. M.; Lindahl, P. A. *Biochemistry* **1994**, *33*, 14339−14349.
(10) Roberts, L. M.; Lindahl, P. A. *J. Am. Chem. Soc.* **1995**, *117*, 2565−2572.
(11) Teixeira, M.; Moura, I.; Xavier, A. V.; Moura, J. J. G.; LeGall, J.; DerVartanian, D. V.; Peck, H. D., Jr.; Huynh, B.-H. *J. Biol. Chem.* **1989**, *264*, 16435−16450.
(12) Albracht, S. P. J. *Biochim. Biophys. Acta* **1994**, *1188*, 167−204.
(13) Bagyinka, C.; Whitehead, J. P.; Maroney, M. J. *J. Am. Chem. Soc.* **1993**, *115*, 3576−3585.
(14) Eidsness, M. K.; Sullivan, R. J.; Scott, R. A. In *The Bioinorganic Chemistry of Nickel*; Lancaster, J. R., Jr., Ed.; VCH Verlagsgesellschaft mbH: Weinheim, 1988; pp 83−85.
(15) Krüger, H. J.; Holm, R. H. *J. Am. Chem. Soc.* **1990**, *112*, 2955−2963.
(16) Maroney, M. J. In *Encyclopedia of Inorganic Chemistry*; King, R. B., Ed.; Wiley: Sussex, 1994; pp 2412−2426.
(17) Otwinowski, Z. In *Data Collection and Processing*; Sawyer, L., Isaacs, N. W., Bailey, S., Eds.; DL/SCI/R34, Daresbury Laboratory: Warrington, UK, 1993; pp 55−62.
(18) Brünger, A. In *Crystallographic Computing 4: Techniques and New Technologies*; Isaacs, N. W., Taylor, M. R., Eds.; Clarendon Press: Oxford, 1988; pp 127−140.
(19) Leslie, A. G. W. *ESF/CCP4 Newsletter* **1992**, *27*, 30.
(20) Collaborative Computational Project Number 4. *Acta Crystallogr.* **1994**, *D50*, 760−763.
(21) Navaza, J. *Acta Crystallogr.* **1994**, *A50*, 157−163.
(22) Hendrickson, W. A.; Konnert, J. H. In *Computing in Crystallography*; Diamond, R., Ramaseshan, S., Venkatesan, K., Eds.; Indian Institute of Science: Bangalore, India, 1980; pp 1−23.
(23) Brünger, A. *Nature* **1992**, *355*, 472−475.
(24) Read, R. J. *Acta Crystallogr.* **1986**, *A42*, 140−149.
(25) Vellieux, F. M. D. A. P.; Hunt, J. F.; Roy, S.; Read, R. J. *J. Appl. Cryst.* **1995**, *28*, 347−351.
(26) Jones, T. A. *Methods Enzymol.* **1985**, *115*, 157−171.
(27) Laskowski, R. A.; MacArthur, M. W.; Moss, D. S.; Thornton, J. M. *J. Appl. Cryst.* **1993**, *26*, 283−291.
(28) Cammack, R.; Fernandez, V. M.; Hatchikian, E. C. *Methods Enzymol.* **1994**, *243*, 43−68.

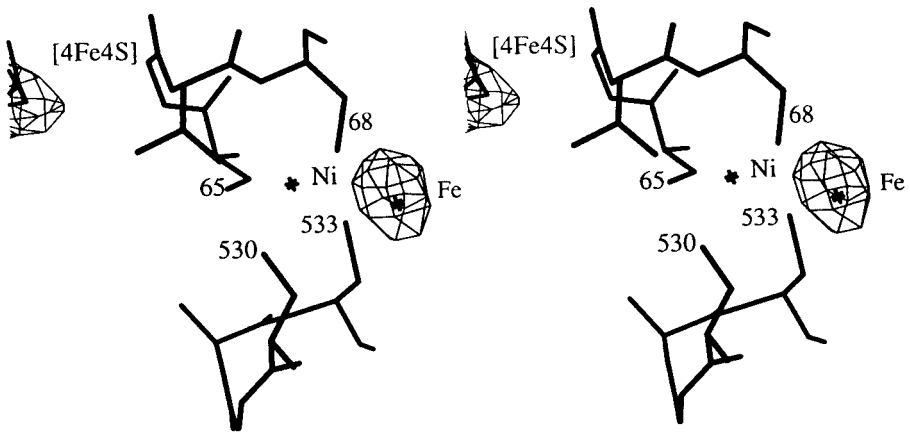

Figure 1. Double difference Δanom(λ_1)−Δanom(λ_2) anomalous map calculated with 90°-shifted phases from the refined λ_1 structure (Table 2). The two wavelengths correspond to the high (λ_1 = 1.733 Å) and low (λ_2 = 1.750 Å) energy sides of the Fe absorption edge. A stereo image of the active site of one of the two molecules is shown with the proximal 4Fe-4S cluster partially included in the upper left corner. Very similar results were obtained for the second molecule in the asymmetric unit.[2] The high electron density peak coincides with the so far unidentified active site metal, providing definite proof that it corresponds to an Fe ion.

Table 2. Refinement Statistics

crystal form	A[b]	B, first[a]	B, final
non-H atoms:	12262	6131	6341
water molecules	0	0	192
resolution (Å)	8.0−3.0	10.0−2.54	8.0−2.54
NF[b]	26973	171548	160306
R (%)[c]	22.1	30.3	20.1
R_{free} (%)	29.4		21.9
σ_{bond} (Å)	0.014	0.012	0.016
σ_{angle} (deg)	2.2	3.4	3.4

[a] Unrefined molecular replacement solution, using the room temperature structure of the first molecule of crystal form. [b] Used observations (no rejections), after excluding 5% of the data (1355 *hkl*'s in form A, 8434 *hkl*'s in form B) for R_{free} calculations. [c] $R = \sum_{hkl}|F_{obs} - F_{calc}|/\sum_{hkl}F_{obs}$.

enzyme concentration was 1.5 mM in 100 mM Tris/KCl buffer, pH 8.1. Activation was performed by putting the sample 2 h under a 100% H_2 atmosphere at 40 °C. The measured activity was 500 μmol H_2 consumed per minute and per mg protein using 1 mM methyl viologen as electron acceptor. The various redox states were generated by controlling the redox potential of the sample using different H_2 pressures, by slow exposure of reduced samples to atmospheric oxygen, as described by Bagley et al.[3] for *C. vinosum* hydrogenase, or by the addition of sodium dithionite. IR frequencies were extracted from spectra that were the average of 1024 scans. Experiments were run in a temperature-controlled Nicolet 5Z-DX FT-IR spectrometer equipped with a gas-tight infrared transmittance cell (sample volume 30 μL, pathlength 60 μm) and CaF_2 windows. The spectral resolution was 2 cm^{-1}. The reference spectrum was the IR cell filled with buffer only. Recorded spectra were baseline-corrected with the program OMNIC from Nicolet.

Results

Crystallographic Identification of Fe in the Active Site. Since a metal content analysis pointed at the presence of 12 (±1) Fe ions in the enzyme,[2] we tentatively assigned the unidentified active site metal to Fe.[2] In order to confirm this hypothesis, two anomalous difference maps were calculated using the data collected on both sides of the Fe absorption edge (λ_1 and λ_2, see Experimental Section), along with 90°-shifted phases from the refined λ_1 model. The "λ_1" map gives significant density for the Fe atoms located in the [3Fe-4S] and the two [4Fe-4S] clusters, and also for the unidentified metal ion in the active site. The "λ_2" map shows only noise at all metal positions. After scaling the two maps to the same r.m.s. (σ) level and subtracting one from the other, the resulting "$\lambda_1-\lambda_2$" difference map shows a highly significant peak (11.3 σ) that coincides with the position of the second active site metal (Figure 1). Since no other significant peaks are found besides the iron-sulfur clusters and the active site, the presence of 12 Fe ions[2] per hydrogenase molecule is confirmed. The present experiment establishes, beyond any reasonable doubt, that the second active site metal ion is iron.

Identification of Ni in the New Crystal Form. A six-fold averaged anomalous difference map of the new pseudo-hexagonal crystal form, calculated with phases from the refined 2.54 Å resolution model shifted by 90°, shows all the cluster metal ions as clearly resolved peaks (Figure 2). The Ni site displays the highest anomalous peak (13.5 σ), whereas the second active site metal gives a peak height of 10.5 σ, comparable to the average peak height of the 11 Fe ions from the [FeS] clusters (10.2 σ). The relative Ni-to-Fe peak heights closely match the f″(Ni) to f″(Fe) ratio at the used wavelength of 0.905 Å (1.704 vs. 1.307 electrons, f″ being the imaginary component of the anomalous scattering factor). These observations indicate that the crystallographic assignment of the Ni position is correct, they confirm that the Ni site is fully occupied, and are also consistent, again, with the assignment of the second active site metal to Fe. Thus the catalytic center of NiFe hydrogenases is heterodinuclear containing Ni and Fe.

Structure of the Active Site in the As-Purified Enzyme. The two active site metals are coordinated by a total of only four protein ligands (Figures 3 and 4). Compared to the previous 2.85 Å resolution analysis of the other crystal form,[2] in the 2.54 Å resolution study of the new form the bridging Cys68 and Cys533 refine to relatively distant positions from the Ni (Table 3). We consider the new distances more reliable in view of the fact that the resolution of the analysis is better and over 10 times more observations per refined parameter were used here. The Fe ion is further coordinated by three completely buried non-protein ligands, which in the 2.85 Å resolution study were included as water molecules; we stated, however, that their actual assignment was not clear.[2,4] Now they have been modeled and refined as diatomic molecules, as neither smaller nor larger ligands can be fitted correctly to the 2.54 Å resolution electron density map. Their assignment will be further discussed below. A strong peak in the six-fold averaged difference ($F_{obs}-F_{calc}$) electron density map (Figure 3) indicates the presence of an additional ligand in a bridging position between the Ni and the Fe centers. We have tentatively assigned this peak to an oxygen species. In summary, the Ni has three close and two distant ligands in a highly distorted square pyramidal conforma-

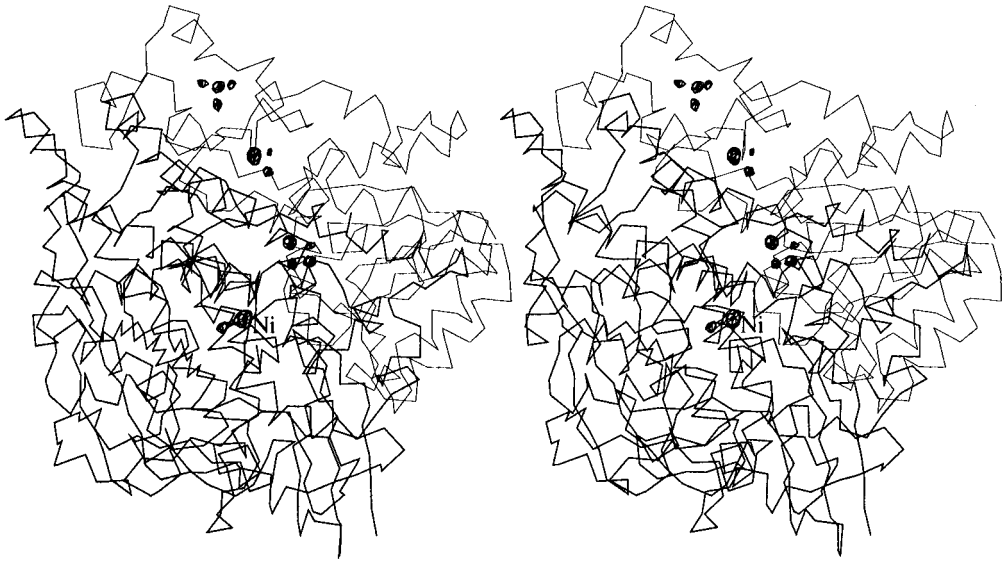

Figure 2. Stereo picture showing the location of Ni and Fe sites in a six-fold averaged anomalous difference map, calculated with phase information from the refined model and approximately 116 000 observed anomalous differences between 20 and 2.54 Å resolution (≈60% completeness) collected at $\lambda = 0.905$ Å. The map is shown at the 8σ level (dark spheres), 1σ being its root mean square value. The Ni peak is labeled. A C^{α} plot of the large (thick lines) and small subunit is also shown.

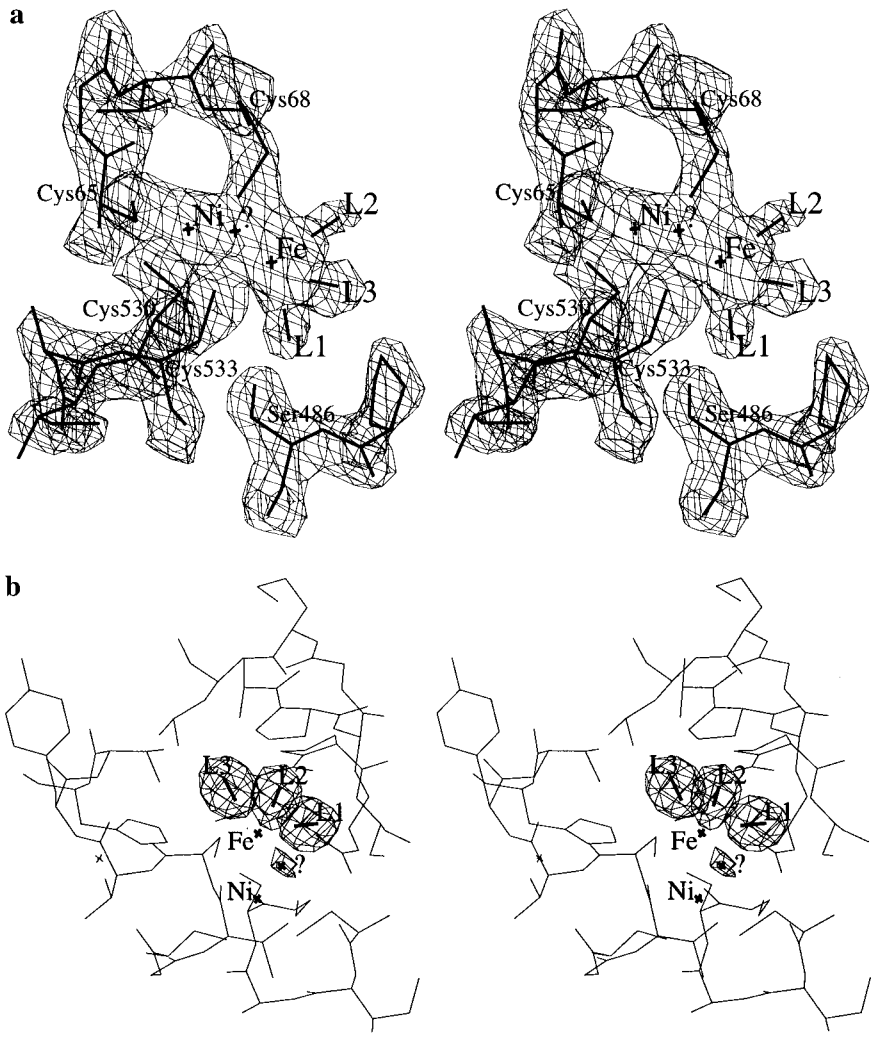

Figure 3. Stereo images of the active site of hydrogenase. Two six-fold averaged maps are shown: (A) calculated with $2mF_o - DF_c$ coefficients[24] and contoured at the 2σ level, with F_c's and phases obtained from the final model. (B) An equivalent $mF_o - F_c$ map in a different orientation, after one cycle of PROLSQ refinement without the contribution of the three putative diatomic ligands (L1−3) and monoatomic bridging ligand (labeled with ?) to the F_c's. Peak heights vary from 5σ for the latter (similar values were observed for water molecules in other omitmaps) to $10-12\ \sigma$ for L1−3, which show more ellipsoidal density shapes. All residues within 7 Å from the Fe are depicted, showing that the special ligands are completely buried. Attempts to refine L1, L2, and L3 as monoatomic S or O gave rise to significantly nonflat final $F_o - F_c$ maps.

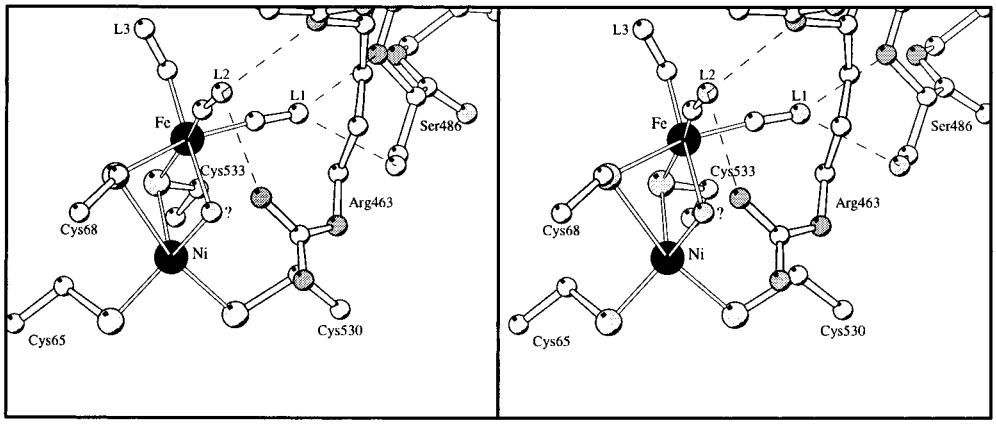

Figure 4. Stereo pair depicting the coordination spheres of the active site metals. Selected bond distances and angles are given in Table 3. The angle between the planes formed by S$^{\gamma}$68, S$^{\gamma}$533, Fe and S$^{\gamma}$68, S$^{\gamma}$533, Ni is 81°. The question mark labels the bridging putative oxygen species. Possible hydrogen bonding interactions involving the diatomic ligands are indicated by dashed lines. Other residues forming part of the active site environment are shown in Figure 3B, which has a similar orientation. This figure was made with the program MOLSCRIPT.[46]

Table 3. Selected Active Site Distances and Angles in the Final Model[a]

atoms	*d* (Å)	atoms	*d* (Å)	atoms	α (deg)	atoms	α (deg)
Ni−S65	2.2	Fe−S68	2.2	S65, Ni, S530	89	C^{L1}, Fe, C^{L2}	94
Ni−S68	2.6	Fe−S533	2.2	S65, Ni, O	154	C^{L1}, Fe, C^{L3}	83
Ni−S530	2.3	Fe−O	2.1	S530, Ni, O	102	C^{L2}, Fe, C^{L3}	91
Ni−S533	2.6	Fe−C^{L1}	1.9	S68, Fe, S533	85	Ni, S68, Fe	74
Ni−O	1.7	Fe−C^{L2}	1.7	S68, Fe, C^{L1}	168	Ni, S533, Fe	74
Ni−Fe	2.9	Fe−C^{L3}	1.9	S533, Fe, C^{L2}	171	Ni, O, Fe	97

[a] The Fe-ligands L1, L2 and L3 were modeled as CO. Weak ligand-distance restraints were used, based on an independent refinement without imposing any geometric restraints for metal−ligand interactions: 1.9 Å for Fe−C and Ni−O, 2.25 Å for Fe−S68, Fe−S533, Ni−S65, and Ni−S530 (σ = 0.05 Å, with refinement weight as $1/\sigma^2$).

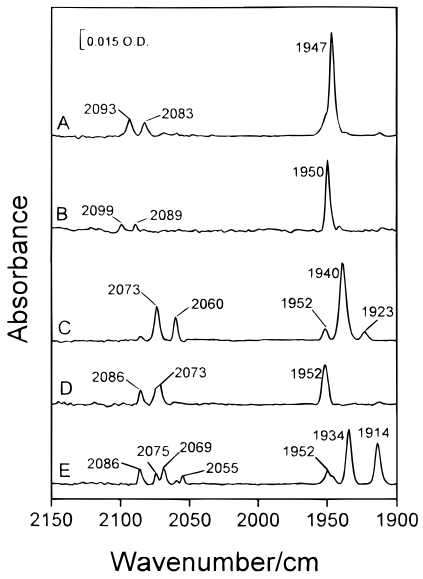

Figure 5. Absolute IR spectra of *Desulfovibrio gigas* hydrogenase in 100 mM Tris/KCl buffer, pH 8.1: (A) 1.25 mM as-purified enzyme at 15 °C. (B) Sample A after addition of 1 mM sodium dithionite at 4 °C. (C) Sample A put under 1 bar of H_2 for 2 hours at 40 °C. (D) Sample C put under 1% H_2. (E) Sample D exposed to air via open filling ports of the IR cell for 65 h.

tion, with a vacant axial sixth ligand site, whereas the Fe has six ligands in a distorted octahedral conformation.

Infrared Spectroscopic Characterization of Seven Redox States. Depending on the redox state of the enzyme, IR spectra of variable complexity are found with bands in the 1900−2100 cm^{-1} frequency region. Spectra corresponding to the EPR-assigned[9,10] redox states Ni−A, Ni−R, Ni−C, and Ni−SI (Figure 5, spectra A, C, D, and E, respectively) were obtained by reductive activation of the as-purified enzyme with molecular hydrogen and subsequent controlled oxidation. These spectra closely resemble those obtained in a similar way from *C. vinosum* hydrogenase.[3] A hitherto unobserved state called Ni−SU (Figure 5B) was found by reduction of Ni−A with 1 mM sodium dithionite at 4 °C. Since at this temperature no activation takes place,[7] we consider this state to correspond to a form that is one electron more reduced than Ni−A and still unactive, i.e. an "unready" partially reduced form. Two sets of three bands were found for Ni−SI, indicating the presence of two distinct states, here called Ni−SI_I and Ni−SI_{II}, as compared to the singlet set of three bands (similar to Ni−SI_I) found in *C. vinosum* hydrogenase.[3]

After a period of 4 days of slow oxidation of the mixture of the two Ni−SI states (Figure 5E), spectrum A of Figure 6 was obtained, indicating the formation of the Ni−B state. This spectrum is different from the one of the as-purified enzyme (that displays mainly Ni−A) and still includes some contribution of the two Ni−SI signals, which disappear after quick exposure to air (Figure 6B). Although the overall appearance of the spectra does not change significantly, the difference spectrum clearly shows that the Ni−SI_I and Ni−SI_{II} species were converted to Ni−A (Figure 6C). From these results we can draw three conclusions: (i) Ni−A and Ni−B have different IR spectra (this is in contrast with *C. vinosum* hydrogenase where no difference was found);[3] (ii) slow oxidation of Ni−SI with air gives mainly Ni−B, whereas fast oxidation gives Ni−A mainly; and (iii) the Ni−B state is stable in the presence of air. Table 4 summarizes the position of the triplets of IR-bands ascribed to each of the seven states identified so far in *D. gigas* hydrogenase. Some minor bands are still unassigned, indicating the possible existence of additional redox intermediates.

Discussion

Assignment of the Diatomic Fe Ligands. Several lines of evidence suggest that the diatomic Fe ligands are responsible for the unusual sets of three IR bands observed in *D. gigas* (Table 4) and *C. vinosum* hydrogenase.[3] (1) These bands are

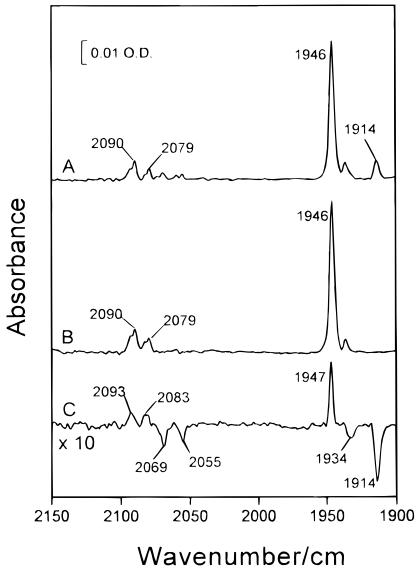

Figure 6. IR spectra of sample E of Figure 5: (A) Absolute spectrum after an additional exposure to air via opened filling ports of the IR cell for 88 hours. (B) Absolute spectrum of sample 6A exposed to air outside the cell. (C) Difference spectrum of 6B−6A.

Table 4. IR Frequencies (cm^{-1}) of the Different Active Site Redox States in *D. gigas* Hydrogenase

redox state	band 1	band 2	band 3	α^a (deg)
Ni−A	1947	2083	2093	89
Ni−B	1946	2079	2090	69
Ni−SU	1950	2089	2099	83
$Ni-SI_I$	1914	2055	2069	71
$Ni-SI_{II}$	1934	2075	2086	60
Ni−C	1952	2073	2086	73
Ni−R	1940	2060	2073	75

[a] The two weaker IR bands (see text) were assumed to be generated by the symmetric (ν_{sym}) and asymmetric (ν_{asym}) stretching vibrations of two coupled oscillators. The angle (α) between these oscillators can be calculated from the ratio of the intensities of ν_{sym} and ν_{asym}.[29]

observed in all the stable redox intermediates, indicating that they arise from intrinsic, nonexchangeable structural features. (2) Their high frequencies (in the 1900−2100 cm^{-1} region) must originate from very strongly bonded species, containing either two subsequent double bonds or a triple bond.[3] (3) The three bands display similar frequency shifts as a function of the redox state of the active site, indicating that they report on electron density changes taking place in their vicinity. (4) No other structural features have been found close to the active site by which such high IR frequencies could be explained.

It should be noted that two of the three IR bands have a much smaller intensity than the remaining one. The frequency difference between the two weaker bands is small (10−14 cm^{-1}) and almost invariable to changes in the redox state of the enzyme. These two bands may be due to the symmetric (ν_{sym}) and asymmetric (ν_{asym}) stretching vibrations of two coupled oscillators. The angle between these oscillators can be calculated from the ratio of the intensities of ν_{sym} and ν_{asym}.[29] In Table 4 the values of the calculated angles between the coupled oscillators are given for each of the characterized redox states of the active site. Such calculation gives a value of 89° for the Ni−A state. This is close to the observed angle between the equatorial ligands L1 and L2 in the crystal structure, which presumably contains mostly Ni−A (Figures 4 and 5A, Table 3).

The protein environment is significantly different for each of the three diatomic ligands (Figure 4). L1 is oriented so that it could accept two hydrogen bonds donated by the peptide NH and the OH group of Ser486. The guanidinium group of Arg463 and its peptide NH group could act as H-bond donors to L2. Whereas L1 and L2 are coplanar with the two cysteic sulphur ligands of the Fe, L3 occupies the apical position trans to the bridging oxygen species. It is surrounded only by hydrophobic residues. The three special ligands are deeply buried inside the protein structure and are, consequently, completely solvent inaccessible and, most likely, nonexchangeable. Thus they probably constitute an integral part of the active site.

Possible candidates for the diatomic Fe ligands are carbon monoxide (CO), cyanide (CN^-), nitrogen oxide (NO), dinitrogen (N_2) and deprotonated acetylene (CCH^-). Respective frequency ranges of ≈1900−2000 cm^{-1} and ≈2030−2150 cm^{-1} are typically observed for CO and for CN^- bound to Fe sites in proteins.[30] The stretching frequencies of nitric oxide (NO) and nitrosonium (NO^+) are 1840 and 2300 cm^{-1}, respectively.[31] NO ligands could therefore be considered if they had substantial NO^+ character. However, since NO^+ is redox active, at negative potentials it should be reduced to neutral NO and a big shift of the IR bands to values much lower than 1900 cm^{-1} should occur.[32] This is not observed here. Although N_2 is a rather uncommon metal ligand in proteins, stretching frequencies in the 1900−2100 cm^{-1} range have been observed in model compounds containing N_2 as a metal ligand,[32] within the range of high IR frequencies observed in hydrogenase. An argument against N_2 stems from its symmetrical nature which should give rise to a small dipole moment upon binding, and, consequently, is not compatible with strong IR signals. The same argument could be used against acetylene.

At this time, it cannot be excluded that the active site Fe actually binds a mixture of different triple-bonded ligands. This is in fact suggested by the marked higher intensity and lower frequency of one of the IR bands relative to the other two. In any case, the presence of three diatomic ligands in the coordination sphere of the active site Fe of hydrogenase, although resembling inorganic model compounds containing CO and/or CN^- complexed to Fe, is without precedent in biological structures. This raises the question of the origin of these special ligands. A recent report suggests that at least one of the many gene products necessary for hydrogenase biosynthesis plays a role in the incorporation of the active site Fe and its non-protein ligands.[33]

Identity of the Small Bridging Ligand. When the reduced, active enzyme is exposed to $^{17}O_2$, broadened EPR spectra are observed for the resulting Ni−A and Ni−B signals,[34] indicating that exogenous oxygen is bound close to the Ni in these states. The only putative exogenous oxygen species close to the Ni that could explain the EPR line broadening is the bridging ligand (Figure 4). At the current resolution of 2.54 Å it cannot be established whether the metal bridging coordination site is partially occupied with either molecular oxygen or peroxide, or fully occupied with a mono-oxygenated species deriving from the reduction of O_2. We favor the latter candidate because it gives an almost featureless ($F_o - F_c$) map around the active site. Also, it would be difficult to include a diatomic molecule because of steric hindrance. Finally, it is unlikely that either

(29) Cotton, F. A.; Wilkinson, G. *Advanced Inorganic Chemistry*; Wiley-Interscience: New-York, 1988; pp 1031−1040.

(30) Nakamoto, K.; Czernuszewicz, R. S. *Methods Enzymol.* **1993**, *226*, 259−289.

(31) Stamler, J. S.; Singel, D. J.; Loscalzo, J. *Science* **1992**, *258*, 1898−1902.

(32) Nakamoto, K. *Infrared and Raman Spectra of Inorganic and Coordination Compounds*; John Wiley and Sons: New York, 1978; pp 259−263.

(33) Rey, L.; Fernandez, D.; Brito, B.; Hernando, Y.; Palacios, J.-M.; Imperial, J.; Ruiz-Argüeso, T. *Mol. Gen. Genet.* **1996**, *252*, 237−248.

(34) Van der Zwaan, J. W.; Coremans, J. M. C. C.; Bouwens, E. C. M.; Albracht, S. P. J. *Biochim. Biophys. Acta* **1990**, *1041*, 101−110.

the Ni−A or the Ni−B state bind dioxygen or peroxide, because both can be obtained by anaerobic oxidation of presumably non-oxygenated species such as Ni−C.[34] Incidentally, the electron density map (Figure 3) does not show any feature indicating oxidation of Ni-bound thiolates to either sulfenate or sulfinate species, proposed models for hydrogenase inactivation by molecular oxygen.[35]

The Redox State(s) of the Active Site in the Crystal Structure. Crystals of freshly prepared aerobically purified hydrogenase contain a mixture of the two EPR-detectable states Ni−A and, in less amounts, Ni−B, and about 50% of material that is EPR-silent with respect to Ni.[2] The IR spectrum of freshly purified enzyme on the other hand shows three bands assignable to the Ni−A state (Table 4, Figure 5), with only minor contributions from other states. In spite of the possible presence of more than one species in the hydrogenase crystal used for X-ray data collection, most of the active site atoms refine to very low temperature factors (Figure 4). Slightly higher temperature factors are found for the Ni ion, the S^{γ}-atom of Cys530 and the bridging putative oxygen species. This could reflect static, rather than dynamic, disorder, since data collection was carried out under cryogenic conditions. We conclude from this that structural differences between the various active site states possibly present in the crystal would concern mainly these three atoms.

Formal Charge of the Ni Ion. EPR studies show that the Ni−A/B/C signals originate from paramagnetic Ni in the active site,[36] which may correspond to either Ni^{3+} or Ni^{+}. Studies of Ni model compounds have shown that Ni^{3+} species could neither bind hydride nor CO, whereas Ni^{+} adducts can.[37] This favors a Ni^{+} assignment to the Ni−C state of hydrogenase, a putative hydride species[38] (see below) that can reversibly bind the competitive inhibitor CO.[12] Careful analysis and modeling of redox titrations have indicated that the Ni−C state is most likely *two electrons* more reduced than the Ni−B state.[9,10] Accordingly, a Ni^{3+} oxidation state has been proposed for the latter, in agreement with other arguments[11] that will not be repeated here. However, if Ni−C is a hydride (or H_2) species, the two electrons would reside in the H^- (H_2) ligand[39] implying that the formal valencies of the active site metal ions do not change upon reduction from Ni−B to Ni−C. Therefore both could contain Ni^{+}. That the Fe ion has the same formal charge is in fact suggested by the similar positions of the three high frequency IR bands (Table 4) in the spectra of these two states (see below). The absence of significant shifts in the Ni K-edge observed in XAS experiments[13] argues against a change of Ni oxidation state (although this interpretation is considered to be controversial by some authors).[9] Also, a formal Ni(I) assignment for Ni−SI (the postulated hydrogen active oxidant)[9] may be considered because in relevant model compounds Ni^{+} adducts are the best catalysts of the heterolytic cleavage of H_2 and form significant amounts of $Ni-H^-$.[40] Since Ni−SI is a diamagnetic species, a Ni(I) assignment for this state requires magnetic coupling with (a redox active) Fe in the active site (see below). A predominant role for Ni^{+} during catalysis in general is also suggested by the observation that bridging thiolates, like the ones found in the active site of hydrogenase, should help stabilize low Ni oxidation states,[41] and by the small number of tightly-bound Ni ligands (Table 3). Finally, at least one of the cysteine ligands of the Ni is likely to become, at least temporarily, protonated after reductive activation and heterolytic cleavage of H_2. Thiolates ligated to Ni^{+} should be easier to protonate than Ni^{3+}-bound ones. Although direct binding of H_2 to Ni−B has not been demonstrated, it is possible to activate crystals of as-purified hydrogenase using molecular hydrogen in the absence of redox mediators.[42]

Substrate Binding to the Active Site. The nature of the catalyzed reaction requires the active site to be able to take up two electrons, presumably as H_2 or H^-. Next, the electrons are likely to be transferred to the hydrogenase redox partner cytochrome c_3 through a pathway that includes the two [4Fe-4S] clusters bound to the small subunit.[2] Since only one electron at a time can be delivered to the proximal [4Fe-4S] cluster, the second one must remain at the active site until this cluster is re-oxidized. If our assignment of the IR bands to the diatomic Fe ligands is correct, then their frequency shifts as a function of active site redox state (Table 4) strongly suggest a significant redox role of the Fe center. Therefore, in the simplest possible scheme, two-electron reductions are attributed to the base-assisted heterolytic cleavage of H_2 by the Ni ion, with concomitant H^- binding (and no formal change in the redox state of both active site metals). Subsequent one-electron oxidations would involve primarily the Fe center.

Considering that the Ni is coordinated by four cysteine ligands, there are two remaining ligation sites that could be available for binding substrate (Figure 4). The equatorial metal bridging site that is occupied by a putative oxygen species in the crystal structure appears to be well suited for binding an anionic species. Its negative charge would be stabilized by the two active site metals and possibly the guanidinium group of Arg463 (Table 5). The putative hydride in Ni−C might therefore replace the bridging ligand observed in the crystal structure, providing a simple model for the reductive activation of the enzyme. In fact, the EPR signal of Ni−C shows a weak hyperfine (J) coupling of 16.8 MHz that could be assigned to bound hydride.[43] Although a higher value might be expected in view of the high magnetic moment of hydrogen, a weak $Ni-H^-$ interaction could be due to additional binding of the hydride to the Fe (Figure 4). Moreover, there are examples of equatorial hydrides in Ni^{+} model compounds that show no hyperfine splitting.[40] Conversely, a strong hyperfine coupling (≈90 MHz) has been observed in the EPR spectrum of the complex formed between ^{13}CO and Ni−C.[34] This may result from CO binding to the axial vacant Ni ligation site which is perpendicular to the equatorial metal bridging site and, consequently, may sense more of the spin density. In addition, the high IR frequency of exogenous CO complexed to *C. vinosum* hydrogenase[44] suggests that this ligand is terminally bound.[3]

The Ni−C EPR signal is known to be light sensitive.[6,38] An ENDOR study of the Ni−C signal in *T. roseopersicina* hydrogenase suggested that the disappearance of hyperfine coupling when the sample was illuminated resulted from the photodissociation of either a proton, a hydride or molecular hydrogen from the Ni center.[45] When the same process was

(35) Kumar, M.; Colpas, G. J.; Day, R. O.; Maroney, M. J. *J. Am. Chem. Soc.* **1989**, *111*, 8323−8325.
(36) Moura, J. J. G.; Moura, I.; Huynh, B. H.; Krüger, H.-J.; Teixeira, M.; DuVarney, R. G.; DerVartanian, D. G.; Ljungdahl, P.; Xavier, A. V.; Peck, H. D., Jr.; LeGall, J. *Biochem. Biophys. Res. Commun.* **1992**, *108*, 1388−1393.
(37) Marganian, C. A.; Vazir, H.; Baidya, N.; Olmstead, M. M.; Mascharak, P. K. *J. Am. Chem. Soc.* **1995**, *117*, 1584−1594.
(38) Van der Zwaan, J. W.; Albracht, S. P. J.; Fontijn, R. D.; Slater, E. C. *FEBS Lett.* **1985**, *179*, 271−277.
(39) Collman, J. P. *Nature Struct. Biol.* **1996**, *3*, 213−217.
(40) Marganian Goldman, C.; Mascharak, P. K. *Comments Inorg. Chem.* **1985**, *18*, 1−25.
(41) Farmer, P. J.; Reibenspies, J. H.; Lindahl, P. A.; Darensbourg, M. Y. *J. Am. Chem. Soc.* **1993**, *115*, 4665−4674.
(42) Nivière, V.; Hatchikian, C.; Cambillau, C.; Frey, M. *J. Mol. Biol.* **1987**, *195*, 969−971.
(43) Fan, C.; Teixeira, M.; Moura, J.; Moura, I.; Huynh, B. H.; LeGall, J.; Peck, H. D. J.; Hoffman, B. M. *J. Am. Chem. Soc.* **1991**, *113*, 20−24.
(44) Bagley, K. A.; Van Garderen, C. J.; Chen, M.; Duin, E. C.; Albracht, S. P. J.; Woodruff, W. H. *Biochemistry* **1994**, *33*, 9226−9236.
(45) Whitehead, J. P.; Gurbiel, R. J.; Bagyinka, C.; Hoffman, B. M.; Maroney, M. J. *J. Am. Chem. Soc.* **1993**, *115*, 5629−5635.

studied by IR spectroscopy using hydrogenase from *C. vinosum*, exposure to light induced large shifts of the three special IR bands to lower frequencies.[3] These results suggest that light induced a change of electron density at the Fe center. Taken together, the EPR and IR results could be conciled if, upon illumination, the putative bridging hydride changed into a terminal Fe-bound hydride. This would require relatively minor changes, which is attractive since the hydrogenase active site is completely buried in the protein core and, consequently, is unlikely to undergo major structural rearrangements.

The Magnetic States of the Active Site through the Catalytic Cycle. Our discovery that the active site is binuclear,[2] the results reported here concerning the unambiguous identification of the second metal site as Fe, and the redox-dependent shifts of the high frequency IR bands suggest that the active site Fe center is redox-active. Since the EPR studies provide no indication for the presence of a nearby paramagnet close to the Ni, the active site Fe ion is most probably diamagnetic in the Ni−A/B/C states. This requires a low-spin Fe^{2+} formal oxidation state, which is normally only observed in a strong octahedral ligand field. The proposed assignment of three diatomic ligands that could be CO and/or CN^-, to the Fe coordination sphere is consistent with the Fe being low-spin. If, as suggested above, the catalytic nickel is Ni^+ in many, if not all, the relevant redox states, a strong magnetic coupling of the two metals would be required in order to explain the EPR-silent Ni−SI and Ni−R states. These would then have either Ni^+/Fe^+ or Ni^+/Fe^{3+} formal oxidation states. If the Ni is involved in one-electron redox chemistry, a diamagnetic Ni^{2+}/Fe^{2+} couple may exist instead. These would also be the preferred metal oxidation states if redox active thiyl radicals are involved.[16] Alternatively, both the Ni−SI and Ni−R states might contribute to a very low field EPR signal which has been found to exist at all redox potentials where the enzyme is active. This signal has been proposed to arise from a change in the electronic state of the reduced [3Fe-4S] cluster.[11] Clearly, more studies will be required before a definitive explanation is found.

Possible Catalytic Mechanisms. Assuming there is a bound hydride in Ni−C, two possible mechanisms can be formulated for its one-electron oxidation to Ni−SI: either the formal oxidation state of the Fe is raised by one, with a remaining bound hydride, or the hydride is cleaved by the removal of one of its two electrons, after which the second electron may reduce the Fe center. As shown in Figure 7, different electronic configurations are, in principle, possible for Ni−SI. The crystal structure is compatible with the two possible schemes proposed in that figure. What would be the effects of a possible mixture of CO, CN^- and/or other triple-bonded ligands on the redox behavior of the Fe center is not immediately obvious. An intriguing question is: how many hydrides are formed during catalysis?

If the electron density at the Fe center is the main factor determining the frequency of the IR bands assigned to the diatomic Fe ligands, their shifts to lower values in the Ni−SI and Ni−R states suggest an increased back donation from the metal,[30] consistent with a more electron-rich Fe, such as Fe^+. However, π back bonding can also be increased by factors like the addition of strong donors, such as hydride, and stronger

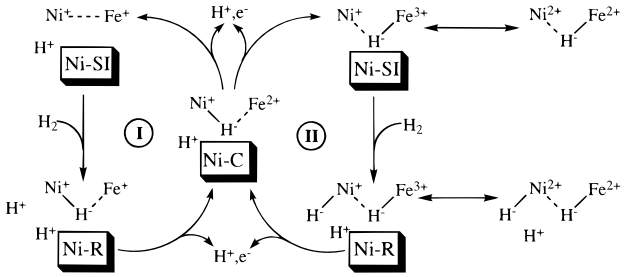

Figure 7. Possible H_2 oxidation cycles (marked I and II) in *D. gigas* hydrogenase. The central assumption is that the bridging putative oxygen species observed in the crystal occupies the position of a hydride in the Ni−C state (see text). States shown on the same line are both isoelectronic and isoprotonic. For simplicity, only the active site metal ions and those hydrogen species that may be directly involved in catalysis are shown. Because the present study presents evidence for the existence of two distinct Ni−SI states (see text) which probably differ in their protonation state (our own unpublished results), the extra protonation step postulated to occur in the Ni−SI to Ni−C transition[6] is not included here.

hydrogen bonding between metal ligand and protein.[30,32] The concept of formal charges is complicated by the significant covalent character of metal to ligand bonds, and it is probably better to regard the charge of the metal center as a whole, including the ligands. Therefore the formation of (formal) Fe^{3+}-hydride complexes in one or more of the Ni EPR-silent states, as the ones shown in Figure 7, may have to be considered. Since the IR data suggest the existence of more states than the ones expected from EPR studies alone, more structural and spectroscopic data will have to be gathered before a comprehensive picture concerning the electronic configuration of the active site of [NiFe] hydrogenases during activation and catalysis emerges.

Concluding Remarks

One of the next challenges will be the chemical determination of the identity of the diatomic Fe ligands. In this respect, higher resolution crystallographic studies will help, but probably cannot solve the issue. The definite answer will most likely come from isotopic substitution studies with ^{13}C, ^{15}N and/or ^{17}O, using IR spectroscopy to study the resulting species, and from the characterization of putative gene products involved in hydrogenase maturation. X-ray crystallographic analyses of anaerobically oxidized (Ni−B), fully reduced (Ni−R), and CO-complexed hydrogenase, as well as IR redox titrations are underway. These studies will help us characterize the structural changes taking place at the active site during activation and catalysis and will provide an indirect view of the substrate binding site.

Acknowledgment. We thank Marie-Hélène Charon for advice concerning the crystallization of hydrogenase. We thank Nicole Forget for her assistance in the purification of the enzyme. The help of Bjarne Rasmussen (beam line 4) and Andrew Thompson (beam line 19) during X-ray data collection at the European Synchrotron Radiation Facility in Grenoble, France, is greatly appreciated. This work was supported by Grant BIO2-CT94-2041 from the European Commission Biotechnology Program, by Grant BIO95-1220-CE from the Spanish CIYT, and by the CEA and the CNRS.

JA962270G

(46) Kraulis, P. *J. Appl. Crystallogr.* **1991**, *24*, 949−950.